**Supplementary Material**

# Tumor MHC Expression Guides First-Line Immunotherapy Selection in Melanoma

**Elena Shklovskaya, Jenny H Lee, Su Yin Lim, Ashleigh Stewart, Bernadette Pedersen, Peter Ferguson, Robyn PM Saw, John F Thompson, Brindha Shivalingam, Matteo S Carlino, Richard A Scolyer, Alexander M Menzies, Georgina V Long, Richard F Kefford and Helen Rizos**

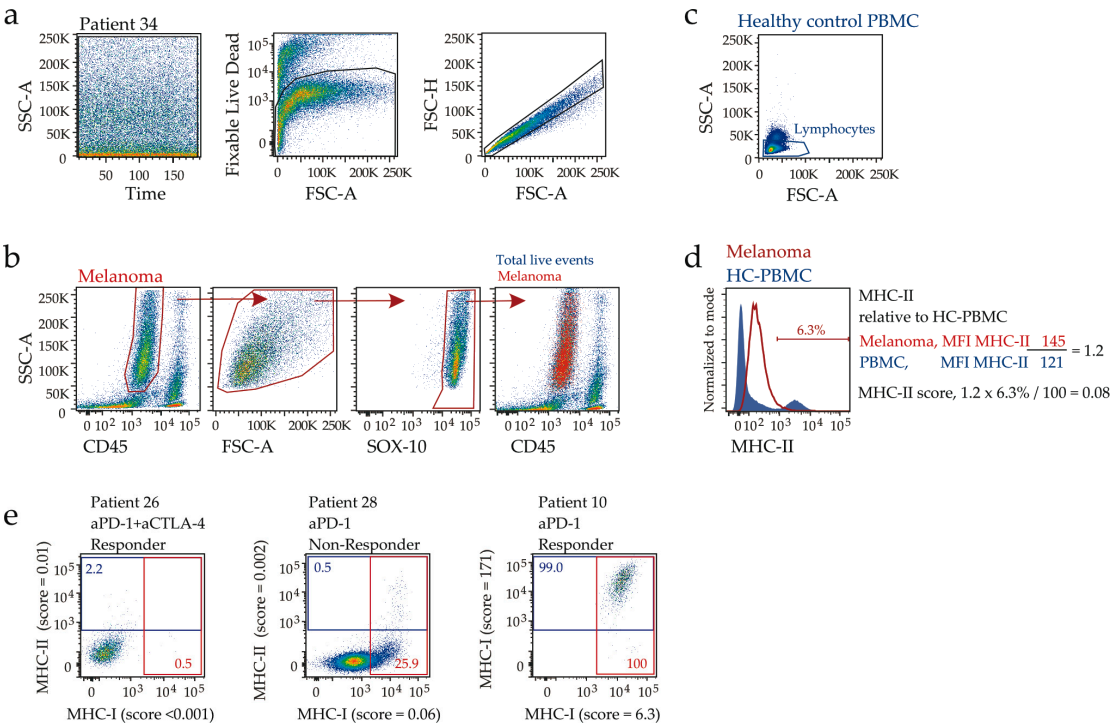


**Figure S1.** Flow cytometric analysis of melanoma cells in enzymatically dissociated tumor biopsies. (**a**) General gating (left to right): time gate, live cell gate, single cell gate. (**b**) Melanoma cell gating (left to right): CD45-negative, side scatter (SSC-A) high; forward scatter (FCS-A) high; SOX-10 positive; overlay of SOX-10 positive melanoma cells (red) onto total live events (pseudocolor plot). (**c**) Healthy control (HC) PBMC lymphocyte gating (SSC-A and FCS-A low). (**d**) MHC-II expression on tumor cells (red histogram) and control PBMC (blue shaded histogram). Fraction of melanoma cells expressing the marker is indicated. Calculations for melanoma MHC-II expression relative to HC-PBMC, and MHC-II expression score are shown (MFI, geometric mean fluorescent intensity). (**e**) Representative examples of MHC expression in three tumors, with frequency of positive (MHC-I, red; MHC-II, blue) and MHC expression scores indicated. Patient ID, therapy and treatment response are indicated above the plots.

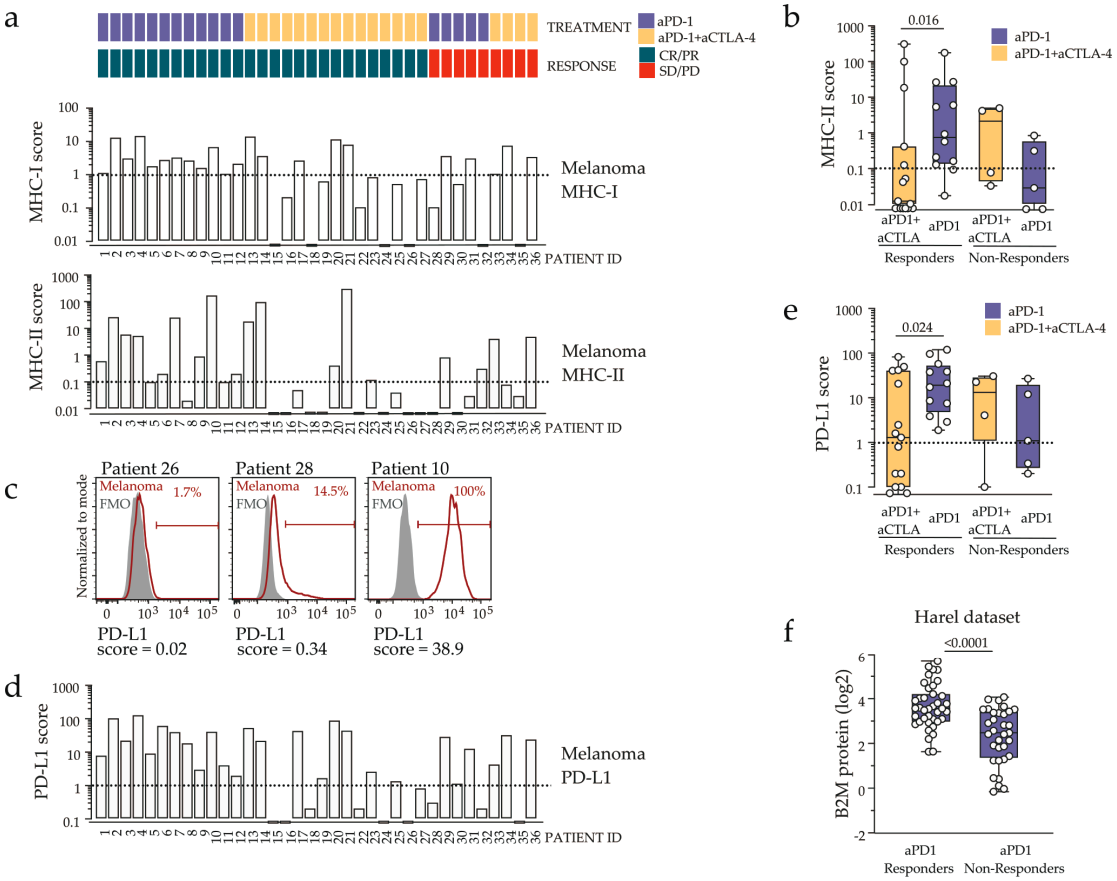


**Figure S2.** Flow cytometric evaluation of tumor MHC-I, MHC-II and PD-L1 expression in pretreatment biopsies. (**a**) Melanoma MHC-I and MHC-II expression scores for the 36 samples included in the study. Treatment, response status and patient ID are indicated. Dotted lines mark expression thresholds. (**b**) Melanoma MHC-II expression score stratified by therapy and patient response. Boxes show the interquartile range and the median, with Mann-Whitney's P values indicated. (**c**) Representative examples of PD-L1 expression for the three biopsies shown in Figure S1E. (**d,e**) Melanoma PD-L1 expression score for the 36 biopsies included in the study (d) stratified by therapy and patient response (e). Boxes show the interquartile range and the median, with Mann-Whitney's P values indicated. (**f**) B2M protein expression in pretreatment biopsies from 39 responders and 33 non-responders to anti-PD-1 monotherapy (Harel dataset, high-resolution liquid chromatography-mass spectrometry data after filtration for 70% valid values [1]). Mann-Whitney's P value is shown.

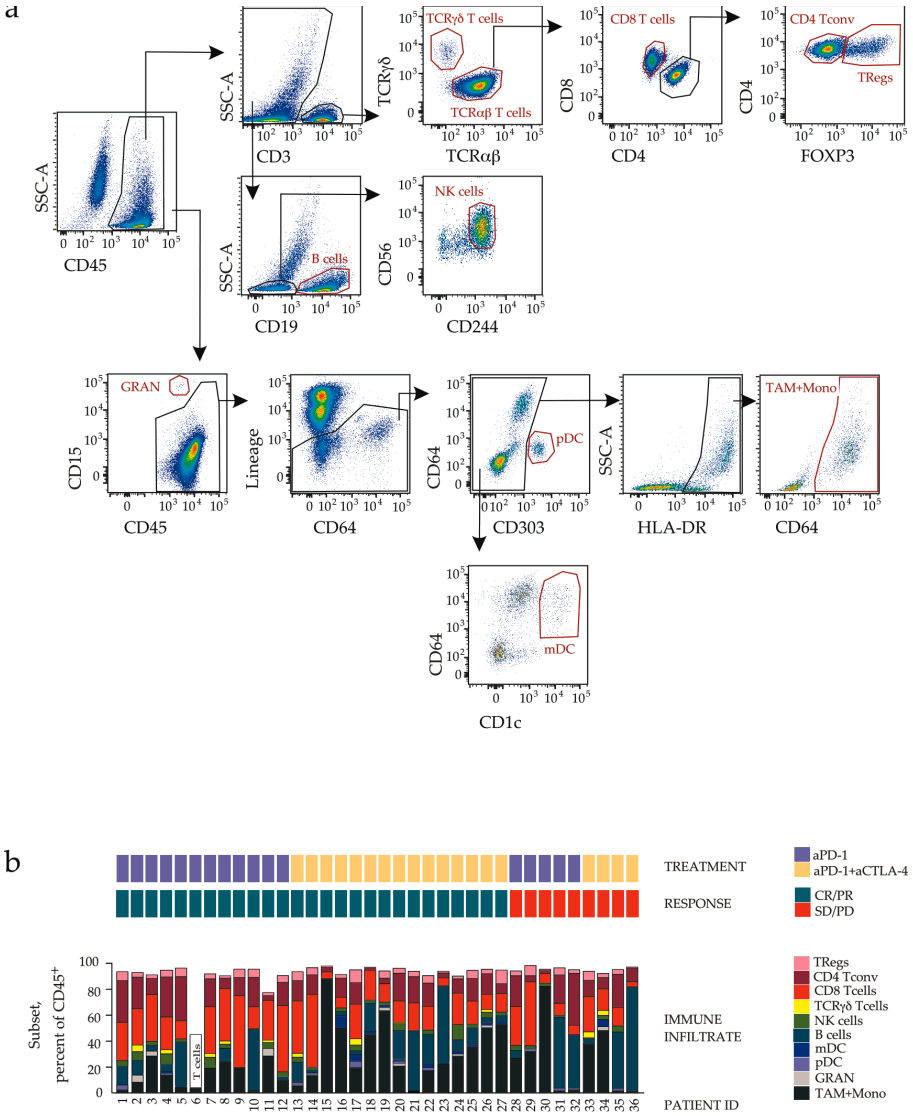


**Figure S3.** Immune contexture of individual melanoma biopsies. (**a**) Identification of tumor-infiltrating immune cells by flow cytometry. After gating CD45$^+$ events, lymphocytes were identified as follows (top row, left to right): SSC-A$^{low}$CD3$^+$ T-cells; TCRγδ$^+$ T-cells, and TCRαβ$^+$ T-cells further gated for CD8$^+$ T-cells, Tconv (conventional CD4$^+$FOXP3$^-$ T-cells) and TRegs (regulatory CD4$^+$FOXP3$^+$ T-cells); (second row): CD3-negatve events were gated for SSC-A$^{low}$CD19$^+$ B-cells, and SSC-A$^{low}$CD3$^{neg}$CD19$^{neg}$ events were gated for CD244$^+$CD56$^+$ natural killer (NK) cells. (Third row, left to right): Alternatively, CD45$^+$ events were gated for CD15$^+$CD45$^{int}$ granulocytes (GRAN). Lineage-negative events (CD3$^-$CD19$^-$CD56$^-$) were further gated for CD303$^+$ plasmacytoid dendritic cells (pDC), HLA-DR$^+$CD1c$^+$ myeloid dendritic cells (mDC) or HLA-DR$^{+/int}$CD64$^+$SSC-A$^{high/int}$ tumor-associated macrophages and monocytes (TAM+Mono). Final gates for individual subsets are shown in red; general gating strategy (Figure S1a) was applied prior to gating. (**b**) Cellular composition of tumor microenvironment in all pretreatment biopsies shown as a fraction of CD45$^+$ cells. Limited analysis was performed for patient 6 due to insufficient material.

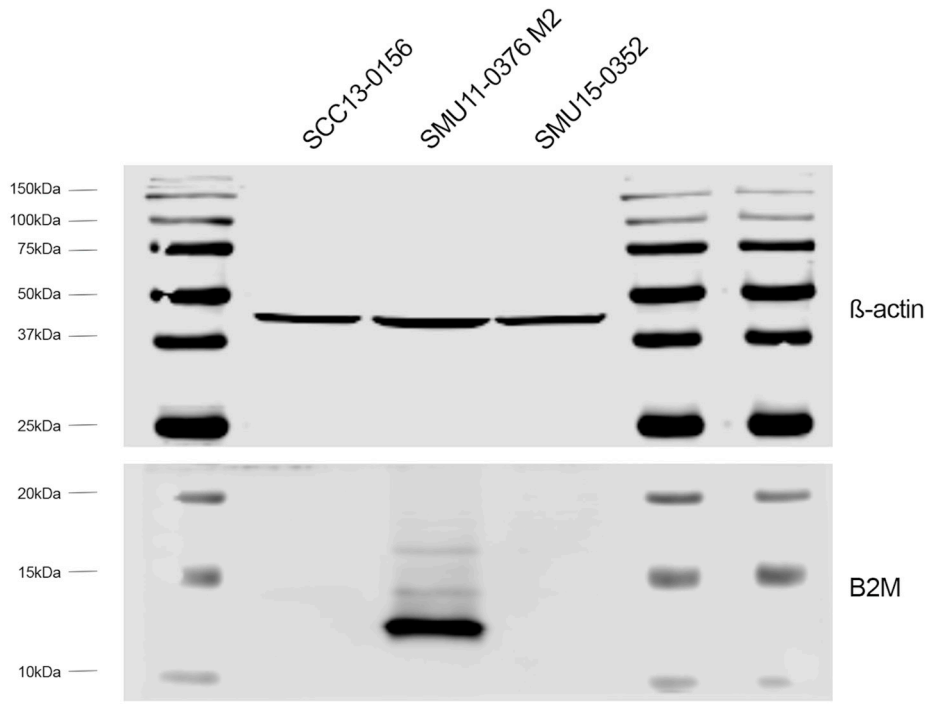


**Figure S4.** Uncropped images for Western blot gels used in Figure 1d.

**Table S1.** Antibodies and reagents used for flow cytometry.

| Marker | Fluorescence | Company | Catalogue |
|---|---|---|---|
| CD1c/BDCA-1 | PECy7 | BioLegend | 331516 |
| CD3 | BUV737 | BD Biosciences | 564308 |
| CD3 | BV786 | BD Biosciences | 565491 |
| CD4 | FITC | BioLegend | 344604 |
| CD4 | AF700 | BioLegend | 357418 |
| CD8 | V500 | BD Biosciences | 561617 |
| CD14 | V500 | BD Biosciences | 561392 |
| CD15 | BV786 | BD Biosciences | 741013 |
| CD16 | AF700 | BD Biosciences | 557920 |
| CD19 | BUV737 | BD Biosciences | 564304 |
| CD56 | PE | Miltenyi Biotech | 130–113–874 |
| CD56 | BUV737 | BD Biosciences | 564448 |
| CD64 | PE | BioLegend | 305007 |
| CD45 | BV711 | BioLegend | 304050 |
| CD45 | BUV395 | BD Biosciences | 563792 |
| CD45RO | BUV395 | BD Biosciences | 564291 |
| CD45RA | BUV737 | BD Biosciences | 564442 |
| CD134/OX40 | PE-Cy7 | BD Biosciences | 563663 |
| CD137/4-1BB | PE-Dazzle 594 | BioLegend | 309826 |
| CD141 | PE-Dazzle 594 | BioLegend | 344120 |
| CD146/MCAM | PE-CF594 | BD Horizon | 564327 |
| CD223/LAG3 | PE | Miltenyi Biotech | 130-105-452 |
| CD244 | PE-Cy7 | BioLegend | 329520 |
| CD357/GITR | BV421 | BD Biosciences | 566423 |
| CD271/NGFR | PE-Cy7 | BioLegend | 345110 |
| CD273/PD-L2 | APC | BioLegend | 329608 |
| CD274/PD-L1 | BV421 | BioLegend | 329714 |
| CD278/ICOS | APC | BioLegend | 313510 |
| CD279/PD1 | BV421 | BD Biosciences | 562516 |
| CD303 | BV421 | BD Biosciences | 566427 |
| CD366/TIM3 | BV786 | BD Biosciences | 742857 |

| | | | |
|---|---|---|---|
| EOMES | PE-Cy7 | Thermo Fisher Scientific | 25–4877–42 |
| FC block | | BD Biosciences | 564220 |
| FOXP3 | PE-CF594 | BD Biosciences | 7235501 |
| FOXP3 | AF488 | BioLegend | 320212 |
| Granzyme B | AF700 | BD Biosciences | 560213 |
| HLA-A, B, C | AF700 | BioLegend | 311438 |
| HLA-DR, DP, DQ | BUV395 | BD Biociences | 740302 |
| KI67 | APC | Thermo Fisher Scientific | 17–5699–42 |
| anti-human IgG4-Fc | PE | Southern Biotech | 9200–09 |
| Sox10 | AF488 | Santa Cruz | sc-365692 AF488 |
| TBET | BV421 | BD Biosciences | 563318 |
| TCR $\alpha\beta$ | APC | BioLegend | 306718 |
| TCR $\gamma\delta$ | BV421 | BD Biosciences | 744870 |
| TIGIT/VSTM3 | PE-Cy7 | BioLegend | 372714 |
| LVE/DEAD Fixable | NIR | ThermoFisher Scientific | L10119 |

## References

1. Harel M., Ortenberg R., Varanasi S.K., Mangalhara K.C., Mardamshina M., Markovits E., *et al.* Proteomics of Melanoma Response to Immunotherapy Reveals Mitochondrial Dependence. *Cell* **2019**; *179*: 236–250 e18.